Tissue-Specific Apocarotenoid Glycosylation Contributes to Carotenoid Homeostasis in Arabidopsis Leaves[1]

Kira Lätari, Florian Wüst, Michaela Hübner, Patrick Schaub, Kim Gabriele Beisel, Shizue Matsubara, Peter Beyer, and Ralf Welsch*

Faculty of Biology II, University of Freiburg, D–79104 Freiburg, Germany (K.L., F.W., M.H., P.S., P.B., R.W.); and Institute of Bio- and Geosciences,: Pflanzenwissenschaften, Forschungszentrum Jülich, D–52425 Juelich, Germany (K.G.B., S.M.)

ORCID IDs: 0000-0003-0973-891X (K.L.); 0000-0002-9941-5550 (F.W.); 0000-0002-8529-4161 (P.S.); 0000-0003-4961-652X (K.G.B.); 0000-0002-2865-2743 (R.W.).

Attaining defined steady-state carotenoid levels requires balancing of the rates governing their synthesis and metabolism. Phytoene formation mediated by phytoene synthase (PSY) is rate limiting in the biosynthesis of carotenoids, whereas carotenoid catabolism involves a multitude of nonenzymatic and enzymatic processes. We investigated carotenoid and apocarotenoid formation in Arabidopsis (*Arabidopsis thaliana*) in response to enhanced pathway flux upon *PSY* overexpression. This resulted in a dramatic accumulation of mainly β-carotene in roots and nongreen calli, whereas carotenoids remained unchanged in leaves. We show that, in chloroplasts, surplus PSY was partially soluble, localized in the stroma and, therefore, inactive, whereas the membrane-bound portion mediated a doubling of phytoene synthesis rates. Increased pathway flux was not compensated by enhanced generation of long-chain apocarotenals but resulted in higher levels of C_{13} apocarotenoid glycosides (AGs). Using mutant lines deficient in carotenoid cleavage dioxygenases (CCDs), we identified CCD4 as being mainly responsible for the majority of AGs formed. Moreover, changed AG patterns in the carotene hydroxylase mutants *lutein deficient1* (*lut1*) and *lut5* exhibiting altered leaf carotenoids allowed us to define specific xanthophyll species as precursors for the apocarotenoid aglycons detected. In contrast to leaves, carotenoid hyperaccumulating roots contained higher levels of β-carotene-derived apocarotenals, whereas AGs were absent. These contrasting responses are associated with tissue-specific capacities to synthesize xanthophylls, which thus determine the modes of carotenoid accumulation and apocarotenoid formation.

In plants, the synthesis of carotenoids is plastid localized, with the plastid type determining their function (Ruiz-Sola and Rodríguez-Concepción, 2012; Nisar et al., 2015). In nonphotosynthetic chromoplasts, carotenoids and their volatile derivatives attract pollinating insects or zoochoric animals. Here, carotenoids are sequestered in diverse suborganellar structures, which can be tubulous, globulous, membranous, or crystalline (Sitte et al., 1980; Egea et al., 2010). In chloroplasts, carotenoids are present in light-harvesting complex proteins and photosynthetic reaction centers. They extend the light spectrum used for photosynthetic energy transformation and act photoprotectively because of their ability to quench excitation energy from singlet- or triplet-state chlorophylls, thereby decreasing the risk that singlet oxygen forms (Niyogi, 1999; Demmig-Adams and Adams, 2002). Furthermore, the regulated epoxidation and deepoxidation of zeaxanthin in the xanthophyll cycle contribute to the nonphotochemical quenching of energy (Niyogi, 1999; Ballottari et al., 2014). In contrast to these processes, which maintain carotenoid integrity, carotenoids are also capable of chemically quenching singlet oxygen by their own oxidation, which is accompanied by the release of various carotenoid degradation products (Ramel et al., 2012a, 2013).

The various functions of carotenoids require their dynamic qualitative and quantitative tuning in response to environmental conditions to attain and maintain adequate steady-state concentrations. These include both the regulation of their synthesis and the formation, release, or disposal of their breakdown products. The synthesis of carotenoids is initiated by the condensation of two molecules of geranylgeranyl diphosphate to form phytoene catalyzed by the enzyme phytoene synthase (PSY), which is considered as the rate-limiting enzyme (von Lintig et al., 1997; Li et al., 2008; Rodríguez-Villalón et al.,

[1] This work was supported by the HarvestPlus Research Consortium and the Deutsche Forschungsgemeinschaft (research grant no. WE4731/2–1 to R.W.).

* Address correspondence to ralf.welsch@biologie.uni-freiburg.de.

The author responsible for distribution of materials integral to the findings presented in this article in accordance with the policy described in the Instructions for Authors (www.plantphysiol.org) is: Ralf Welsch (ralf.welsch@biologie.uni-freiburg.de).

K.L., F.W., M.H., and P.S. performed most of the experiments; K.G.B. and S.M. designed and performed the ^{14}C-labeling experiments; P.B. and R.W. designed the other experiments, analyzed the data, and wrote the article; all authors read and approved the final version of the article.

www.plantphysiol.org/cgi/doi/10.1104/pp.15.00243

2009; Welsch et al., 2010; Zhou et al., 2015). In plants, two desaturases, phytoene desaturase and ζ-carotene desaturase, and two carotene cis-trans-isomerases convert the colorless phytoene into the red-colored all-trans-lycopene (Isaacson et al., 2002; Park et al., 2002; Chen et al., 2010; Yu et al., 2011). Two lycopene cyclases introduce either β- or ε-ionone rings, yielding α-(ε,β-)-carotene and β-(β,β)-carotene. In Arabidopsis (*Arabidopsis thaliana*), four enzymes hydroxylate carotenes with partially overlapping substrate specificity (Kim et al., 2009). Two nonheme iron-dependent β-carotene hydroxylases (BCH), BCH1 and BCH2, convert β-carotene into zeaxanthin. The second set of hydroxylases, cytochrome P450 (CYP)97A3 and CYP97C1, prefers α-carotene and produces zeinoxanthin and lutein, respectively. Absence of each cytochrome P450 hydroxylase constitutes a distinct phenotype, named *lutein deficient5* (*lut5*) for CYP97A3 deficiency and *lut1* for CYP97C1 deficiency, characterized by altered pigment compositions and the accumulation of monohydroxylated intermediates, whereas deficiency in BCH1 and BCH2 does not affect the pigment composition.

In green tissues, photooxidative destruction seemingly predominates and consumes carotenoids (Simkin et al., 2003). Moreover, $^{14}CO_2$ pulse-chase experiments with Arabidopsis leaves identified α- and β-carotene as the main targets for photooxidation, whereas xanthophylls were less affected (Beisel et al., 2010). Oxidation assays with β-carotene showed epoxy- and peroxy-derivatives as the main primary products, which however, undergo additional reactions, yielding more stable degradation products that are, in part, the same apocarotenals/ones as those being produced enzymatically (Ramel et al., 2012a, 2013).

In Arabidopsis, genes coding for carotenoid cleaving enzymes (*carotenoid cleavage dioxygenases* [*CCDs*]) form a small gene family comprising nine members, five of which are attributed to the synthesis of abscisic acid (ABA; nine-cis-epoxycarotenoid cleavage dioxygenases [NCEDs]; AtNCED2, AtNCED3, AtNCED5, AtNCED6, and AtNCED9; Iuchi et al., 2001; Tan et al., 2003), whereas two are committed to strigolactone biosynthesis (CCD7/MORE AXILLARY GROWTH3 [MAX3] and CCD8/MAX4; Alder et al., 2012; Bruno et al., 2014). Orthologs of CCD1 are involved in the generation of volatile apocarotenoids contributing to flower scents and aroma production (e.g. saffron [*Crocus sativus;* Rubio et al., 2008; Frusciante et al., 2014] and tomato [*Solanum lycopersicum*; Simkin et al., 2004]), whereas CCD4 enzymes are involved in citrus peel and chrysanthemum (*Chrysanthemum morifolium*) petal coloration (Ohmiya et al., 2006; Rodrigo et al., 2013). Recent analysis of Arabidopsis mutants revealed a major function of CCD4 in regulating seed carotenoid content with only a minor contribution of CCD1 (Gonzalez-Jorge et al., 2013). Moreover, CCD4 activity was required for the synthesis of an apocarotenoid-derived signaling molecule involved in leaf development and retrograde gene expression (Avendaño-Vázquez et al., 2014).

Elevated carotenoid pathway flux caused by *PSY* overexpression increases carotenoid accumulation in various nongreen tissues, such as tomato fruits, canola (*Brassica napus*) seeds, cassava (*Manihot esculenta*) roots, and rice (*Oryza sativa*) endosperm (Shewmaker et al., 1999; Ye et al., 2000; Fraser et al., 2002; Welsch et al., 2010). Similarly, the constitutive overexpression of *PSY* in Arabidopsis results in dramatically increased carotenoid amounts accumulating as crystals in nongreen tissues, such as roots and callus, yielding β-carotene as the main product (Maass et al., 2009). However, leaves of the very same plants do not show altered pigment composition, and phytoene or other pathway intermediates are not detected. Similarly, increased levels of active PSY protein achieved though overexpression of the ORANGE protein exclusively affect carotenoid amounts in roots but not in leaves (Zhou et al., 2015). Leaves from constitutively *PSY*-overexpressing tomato and tobacco (*Nicotiana tabacum*) plants are also reported to show only slightly increased carotenoid levels compared with the wild-type control (Fray et al., 1995; Busch et al., 2002). These contrasting responses of leaves versus nongreen tissues to elevated pathway flux suggest fundamental differences in the modes of carotenoid formation and/or degradation.

In this work, we identified xanthophyll-derived apocarotenoid glycosides (AGs) in Arabidopsis leaves that increase upon higher pathway flux. This suggests that apocarotenoid glycosylation functions as a valve regulating carotenoid steady-state levels in leaves. The analysis of Arabidopsis mutants enabled us to conclude on potential precursor carotenoids and assess the contribution of carotenoid cleavage enzymes on their formation. Moreover, apocarotenoids but not the identified glycosides were increased in carotenoid-hyperaccumulating roots, indicating tissue-specific different modes of carotenoid turnover regulation.

RESULTS

Carotenoid Pathway Flux and PSY Localization upon Increased PSY Protein Levels

In Arabidopsis roots, the constitutive *AtPSY* overexpression results in an up to 100-fold increased carotenoid accumulation. In contrast, leaves of these lines do not respond and contain carotenoid amounts like the wild type, although PSY protein levels are strongly elevated (Maass et al., 2009). Increased pathway flux might be compensated by higher turnover of leaf carotenoids. Alternatively, overexpressed PSY protein might be enzymatically inactive. To discriminate, we determined the phytoene synthesis rates in detached leaves using the phytoene desaturase inhibitor norflurazon (NFZ) assuming that phytoene exhibits an increased resistance toward degradation processes (Simkin et al., 2003). We followed an established protocol consisting of a 2-h preincubation in the dark followed by a 4-h illumination on NFZ solution (Beisel et al., 2011). Wild-type leaves accumulated about 20 mmol of phytoene per

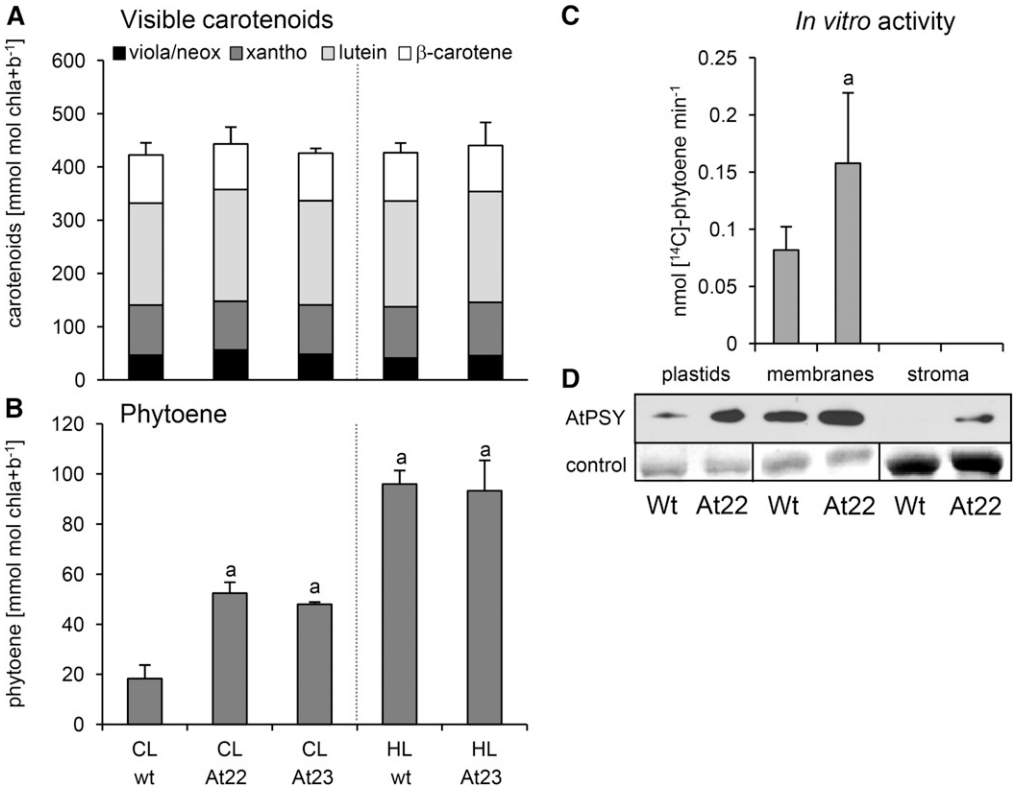

Figure 1. Increased carotenoid pathway flux in leaves of *AtPSY*-overexpressing Arabidopsis lines. Despite similar levels of visible carotenoids (A), phytoene accumulates upon NFZ inhibition in leaves of *AtPSY*-overexpressing lines (At22 and At23) to about 2-fold higher levels compared with the wild type (wt) after 4 h of exposure to control light (CL; B). High light (HL) results in similar phytoene levels in both the wild type and At23. Increased AtPSY amounts in At22 are partially inactivated by stromal localization as shown by immunoblot analysis with whole plastids, membrane and stromal fractions (D), and in vitro [^{14}C]phytoene analysis (C). Bands from a Coomassie-stained SDS gel representing Rubisco large subunit (plastids and stroma) and an abundant light harvesting complex II protein (membranes) are shown as control for equal loading of proteins. Data are mean ± SE of three (A and B) and eight (C) biological replicates. neox, Neoxanthin; viola, violaxanthin; a, significant difference to control samples (Student's *t* test, $P < 0.002$).

1 mol chlorophyll (chl) a + b (or 0.1 μg of phytoene per 1 mg of dry weight) within 4 h of exposure to control light (Fig. 1), whereas high light intensity further increased phytoene levels by 5-fold, reaching 100 mmol of phytoene per 1 mol chl a + b.

NFZ-treated leaves of *AtPSY*-overexpressing lines illuminated with high light accumulated the same high phytoene levels of 100 mmol of phytoene per 1 mol chl a + b. However, the illumination with control light yielded about 50 mmol of phytoene per 1 mol chl a + b, thus 2.5-fold higher levels compared with wild-type leaves. This indicates that higher PSY protein amounts in the transgenics do increase the pathway flux, although leaf steady-state carotenoid levels remain unaffected. At high light intensities, phytoene synthesis is apparently limited by other factors, such as an exhausted precursor pool.

The 2-fold increased phytoene synthesis capacity in *AtPSY*-overexpressing lines contrasts with the much larger up to 20-fold higher PSY protein levels in leaves (Maass et al., 2009) and chloroplast extracts (Fig. 1D). Chloroplast subfractionation revealed that PSY was, in fact, elevated by only about 2-fold in the membranes; the remainder is apparently soluble in the stroma and therefore, inactive. In vitro measurements of PSY activity confirmed an almost 2-fold higher PSY activity in the membrane fractions (0.157 ± 0.062 nmol of [^{14}C]phytoene min^{-1} in At22 versus 0.082 ± 0.02 nmol of [^{14}C]phytoene min^{-1} in the wild type; a thin-layer chromatography scan is supplied in Supplemental Fig. S1), whereas phytoene synthesis was not detectable in stroma fractions (Fig. 1C).

Identification of AGs in Arabidopsis Leaves

An increased pathway flux not leading to higher carotenoid levels suggests increased carotenoid turnover. This is thought to occur predominantly at the β-carotene level as revealed by $^{14}CO_2$ pulse-chase labeling and the abundance of oxidation products derived from β-carotene (Beisel et al., 2010; Ramel et al., 2012a). In leaves of the wild type and *AtPSY*-overexpressing lines, approximately constant β-carotene steady-state levels were confirmed by measuring $^{14}CO_2$ incorporation into β-carotene (Supplemental Fig. S2A). However, levels of long-chain β-carotene degradation products remained

similarly largely unchanged as revealed by the liquid chromatography (LC)-mass spectrometry (MS) analyses of β-apo-14′-carotenal, β-apo-12′-carotenal, β-apo-10′-carotenal, β-apo-8′-carotenal, β-apo-13-carotenone, and retinal (Supplemental Fig. S2B). Moreover, carotenoid-derived short-chain volatiles are not found in Arabidopsis leaves (Aharoni et al., 2003), with the exceptions of β-cyclocitral and β-ionone, which are reported to be generated upon photooxidative stress (Ramel et al., 2012b; Havaux, 2014). We also did not detect these volatiles by gas chromatography (GC)-MS analysis on headspace sampling or by the use of various extraction protocols. We, therefore, resorted to analyzing AGs, which are known from a variety of plants, especially grapevine (*Vitis vinifera*), where they contribute to the aroma (Winterhalter and Schreier, 1995).

An extraction protocol for grapevine was adapted, which included the enzymatic liberation of the aglycons from aqueous extracts followed by GC-MS analysis (Mathieu et al., 2005). This led to the identification of the following four aglycons in Arabidopsis wild-type leaves (the relative peak area percentage is given in parentheses): 3-oxo-α-ionol (apo1; 4%), 3-oxo-α-ionone (apo2; 3%), 3-hydroxy-5,6-epoxy-β-ionone (apo3; 80%), and 6-hydroxy-3-oxo-α-ionone (apo4; 13%). Three of these AGs are also identified in grapevine leaf extracts (variety Müller-Thurgau). The GC-MS traces representing undigested and glycosidase-treated leaf extracts are shown in Figure 2 (details on the identification of these compounds are shown in Supplemental Figs. S3–S6, and their characteristics are summarized in Supplemental Table S1).

Xanthophylls appear as the likely precursors for the aglycons identified; possible precursor-product relationships are shown in Figure 3. The nonhydroxylated apocarotenoid apo2 is probably formed from apo1 upon oxidation of the hydroxyl group after deglycosylation. Direct precursor apo1 may be α-ring hydroxylated xanthophylls, like lutein and the monohydroxylated intermediate α-cryptoxanthin. Alternatively, β-ring hydroxylated xanthophylls, like zeaxanthin, antheraxanthin, and the intermediates β-cryptoxanthin and zeinoxanthin might also serve as precursors, requiring β- to ε-ring conversion upon enzymatic liberation (this being supported by observations

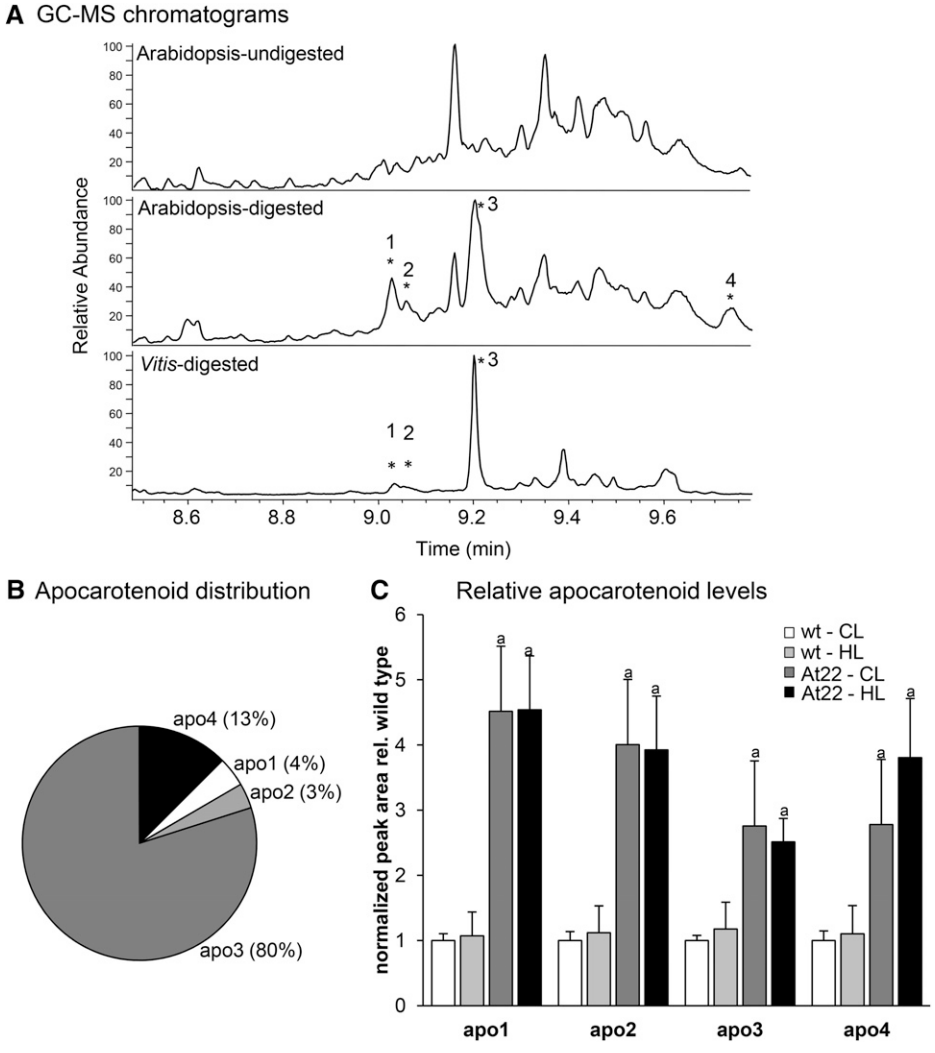

Figure 2. AGs in Arabidopsis leaves. A, GC-MS total ion current chromatograms are shown before (top) and after (middle and bottom) glycosidase digestion of hydrophilic Arabidopsis (top and middle) and *V. vinifera* (bottom) leaf extracts. Four major AGs were determined: apo1 (3-oxo-α-ionole), apo2 (3-oxo-α-ionone), apo3 (3-hydroxy-5,6,-epoxy-β-ionone), and apo4 (6-hydroxy-3-oxo-α-ionone). B, Distribution of single AGs in wild-type leaves (normalized peak areas). C, AGs in leaves of the wild type (wt) and *AtPSY*-overexpressing line At22 grown under control light (CL) and high light (HL). Normalized apocarotenoid levels were expressed relative to wild-type leaves grown under CL. Data are mean ± SE of three biological replicates. No significant difference was detected for the wild type and At22 grown under different light qualities ($P > 0.3$). a, Values that are significantly different from the wild type (Student's *t* test, $P < 0.05$).

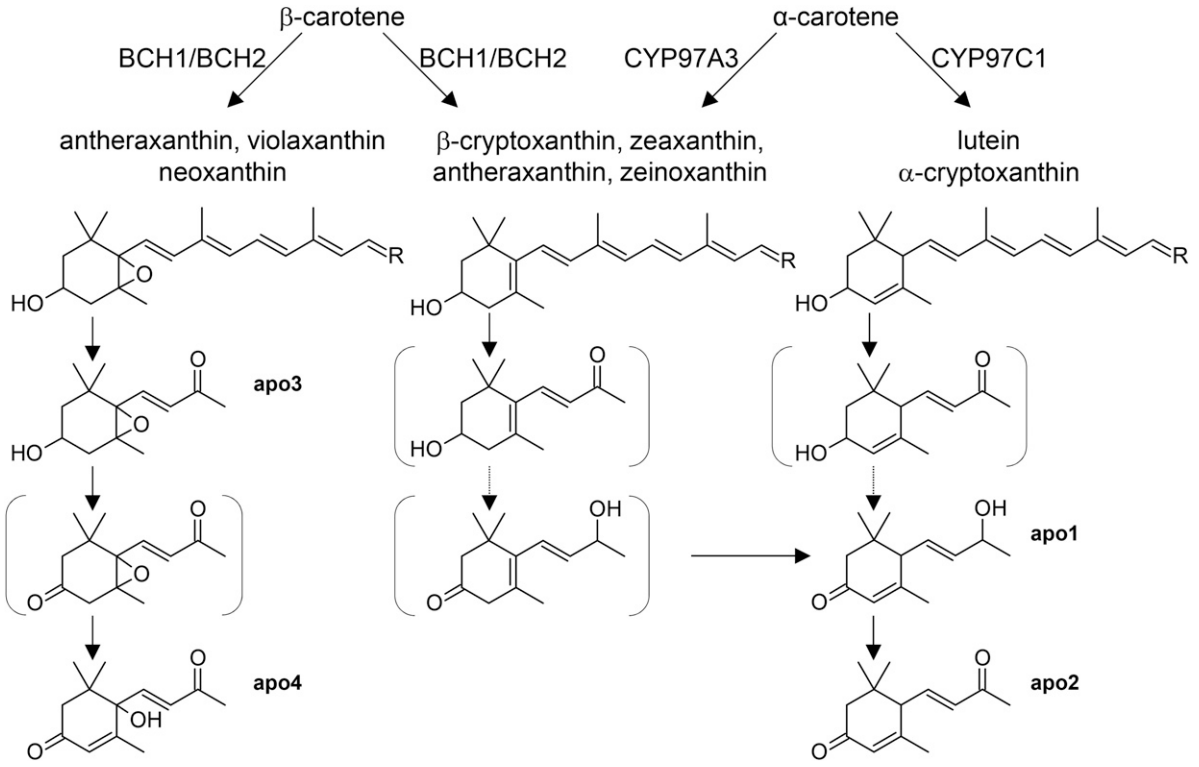

Figure 3. Xanthophyll precursors for AGs in Arabidopsis leaves. AGs identified in Arabidopsis leaves and their possible precursors are shown. Apocarotenoids in brackets were not detected and represent possible intermediates. Only one-half of a xanthophyll molecule is shown; the other one-half is denoted with an R. Carotene hydroxylases with preferences for β-carotene (BCH1 and BCH2) and α-carotene (CYP97A3 and CYP97C1) and derived xanthophylls are indicated.

in grapevine; Mathieu et al., 2009). apo4 probably represents a derivative of apo3 formed upon reduction of the epoxy to a hydroxyl group (Enzell, 1985); apo3 can be formed from epoxyxanthophylls (thus, antheraxantin, violaxanthin, and neoxanthin).

Interestingly, the relative quantification of AGs revealed higher levels in leaves of *AtPSY*-overexpressing lines than in wild-type leaves, which correlates with the increased pathway flux determined above (Fig. 2; GC-MS chromatograms are shown in Supplemental Fig. S7). Hydroxyxanthophyll-derived apocarotenoids (apo1 and apo2) increased about 5-fold, and those derived from epoxyxanthophylls (apo3 and apo4) increased about 3-fold. Considering the reported light stress-induced formation of β-cyclocitral and other carotenoid breakdown products (Ramel et al., 2012b), we further examined a possibly increased apocarotenoid glycosylation under high light stress. However, both wild-type leaves and as well as those from the *AtPSY*-overexpressing line showed no significant changes in their apocarotenoid aglycon levels after 4 h of illumination with 1,500 μmol photons m^{-2} s^{-1}.

Involvement of Enzymatic Carotenoid Breakdown in Apocarotenoid Aglycon Formation

The AGs identified in this work and most of those identified by others in *V. vinifera*, *Boronia megastigma*, and various fruits exhibit a length of ^{13}C atoms (Winterhalter and Skouroumounis, 1997; Mendes-Pinto, 2009; Cooper et al., 2011). AGs with various chain lengths would be expected in case of nonenzymatic carotenoid cleavage. To determine the contribution of enzymatic cleavage, we took advantage of Arabidopsis lines deficient in the carotenoid cleavage enzymes CCD1 and CCD4 (Gonzalez-Jorge et al., 2013), which exhibit a broad substrate specificity (Auldridge et al., 2006; Vogel et al., 2008; Bruno et al., 2015). The carotenoid levels in leaves from 4-week-old plants of *ccd4-1* and a *ccd1-1 ccd4-1* double mutant were similar to the wild type (Table I). However, leaves from both the *ccd4-1* and the *ccd1-1 ccd4-1* mutant showed strongly reduced levels of all AGs, with major reductions in apo3, apo4, and apo1 (Fig. 4; Supplemental Fig. S8 shows GC-MS traces). With apo4 as an exception, there was no significant difference in AG levels comparing the single- and double-mutant lines ($P > 0.25$). The residual presence of apocarotenoid aglycons in *ccd1-1 ccd4-1* leaves thus suggests additional mechanisms yielding the same cleavage products. These results indicate a predominantly enzymatic origin of AGs with a major contribution of CCD4, whereas CCD1 plays a minor role.

Given this role of CCD4 and the constant carotenoid levels in leaves of *AtPSY*-overexpressing lines, we

Table I. *Carotenoid amounts in Arabidopsis mutants*

Carotenoid amounts were determined by HPLC and are given in millimoles moles chl a + b^{-1}. Percentages of carotenoids on total amounts are given in parentheses. Data are means ± SE of three biological replicates. α-caro, α-Carotene; α-crypto, α-cryptoxanthin; anthera, antheraxanthin; β-caro, β-carotene; β-xanthophylls, sum of violaxanthin, antheraxanthin, zeaxanthin, and neoxanthin; moles epoxy, moles of epoxyxanthophyll moieties; n.d., not detectable; viola + neox, sum of violaxanthin and neoxanthin; zeino, zeinoxanthin.

Carotenoid	Columbia-0	*ccd4-1*	*ccd1-1 ccd4-1*	*lut1*	*lut5*
Viola + neox	143.3 ± 9.4 (37)	134.4 ± 9.3 (38)	139.0 ± 17.3 (35)	236.5 ± 33.5 (62)[a]	92.6 ± 4.7 (26)[a]
Anthera	2.5 ± 1.3 (0.6)	2.5 ± 1.4 (0.7)	2.8 ± 0.3 (0.7)	23.3 ± 3.6 (6.1)[a]	3.4 ± 0.7 (1.0)
Zeino	n.d.	n.d.	n.d.	45.0 ± 4.2 (12)[a]	n.d.
α-crypto	n.d.	n.d.	n.d.	n.d.	4.5 ± 0.2 (13)[a]
Other xantho	11.3 ± 2.0 (2.9)	12.2 ± 1.2 (3.4)	13.0 ± 1.6 (3.3)	14.9 ± 2.9 (3.9)	8.9 ± 1.0 (2.5)
Lutein	172.4 ± 13.2 (44)	154.0 ± 16.3 (43)	185.8 ± 7.8 (47)	n.d.[a]	167.9 ± 16.2 (48)
α-caro	3.4 ± 1.1 (0.9)	4.0 ± 1.8 (1.1)	3.2 ± 1.4 (0.8)	4.6 ± 0.9 (1.2)	56.1 ± 3.0 (15.9)[a]
β-caro	55.2 ± 13.7 (14)	50.7 ± 8.2 (14)	54.4 ± 3.3 (14)	60.1 ± 8.4 (16)	18.7 ± 1.8 (5)[a]
Total caro	388.0 ± 23.6	357.8 ± 28.0	398.2 ± 24.3	384.4 ± 52.5	352.0 ± 16.2[a]
β-xanthophylls	157.1 ± 7.3	149.1 ± 10.1	154.8 ± 15.6	274.7 ± 40.0[a]	104.9 ± 5.6[a]
Moles epoxy	289.1 ± 17.8	271.3 ± 18.7	280.9 ± 34.5	496.3 ± 70.6[a]	188.6 ± 9.4[a]

[a]Carotenoids showing significant changes compared with the wild type (Student's *t* test, $P < 0.05$).

challenged flux compensation by crossing *AtPSY*-overexpressing lines with the *ccd4-1* and *ccd1-1 ccd4-1* mutant lines. Although seedlings heterozygous for the *ccd4-1* mutation grew indistinguishable from wild-type plants, individuals homozygous for *ccd4-1* developed light-green cotyledons, which quickly bleached and died. In 1-week-old homozygous seedlings, carotenoid and chlorophyll contents were reduced by about 40% compared with the wild type, and pathway intermediates were not detected (Supplemental Fig. S9). Apparently, formation of xanthophyll breakdown products not formed by cleavage through CCD4 can be tolerated only at physiological pathway fluxes. However, a further increase through higher PSY abundance is lethal, presumably because of the excessive presence of apocarotenoids generated by other mechanisms.

Identification of Xanthophyll Precursors for AGs

We took advantage of the altered leaf xanthophyll patterns found in two Arabidopsis cytochrome P450-type carotene hydroxylase mutants. CYP97C1 catalyzes the hydroxylation of the α-ionone ring present in α-carotene. The respective *lut1* mutant is, therefore, characterized by the absence of lutein and the accumulation of the β-ring monohydroxylated α-carotene-derivative zeinoxanthin (Kim et al., 2009; Table I). The mutant leaves showed about 3-fold increased levels of apo1, whereas other AGs remained unchanged, and no additional AGs were detected (Fig. 4B; Supplemental Fig. S10 shows GC-MS traces). This excludes lutein as a precursor for the AGs identified. In contrast, the increased levels of β-ring hydroxylated xanthophylls in *lut1* leaves suggest zeaxanthin, antheraxanthin, and zeinoxanthin as precursors explaining enhanced levels of apo1.

The second cytochrome P450-type hydroxylase, CYP97A3, catalyzes the hydroxylation of β-ring xanthophylls and prefers α-carotene as substrate but also shows some β-carotene hydroxylation activity. Its absence defines the *lut5* phenotype, which accumulates increased levels of α-carotene accompanied by an almost equivalent reduction of β-carotene. In addition, epoxyxanthophylls, like violaxanthin and neoxanthin, are reduced (Kim and DellaPenna, 2006). In agreement with the suggested origin of apo3 and

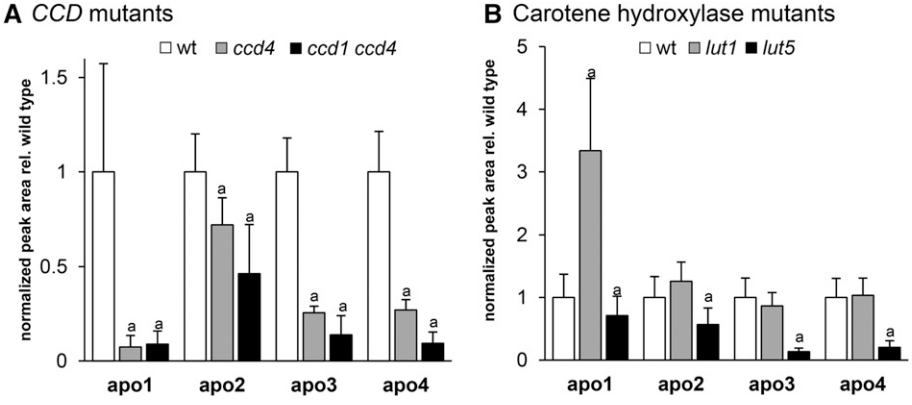

Figure 4. AGs levels in Arabidopsis mutants. AGs in leaves of 4-week-old plants from Arabidopsis wild type (wt; ecotype Columbia-0), *ccd4-1* mutant, and *ccd1-1 ccd4-1* double-mutant lines (A) as well as mutants deficient in carotene hydroxylase (CYP97C1 [*lut1*] and CYP97A3 [*lut5*]; B). Normalized apocarotenoid levels were expressed relative to those in wild-type leaves in each set. Data are mean ± SE of three biological replicates. a, Values that are significantly different from the wild type (Student's *t* test, $P < 0.05$).

apo4 from epoxyxanthophylls (Fig. 3), leaves of *lut5* had strongly reduced levels of these two AGs, whereas those with a suggested origin from hydroxylated xanthophylls decreased only slightly. Furthermore, both epoxyxanthophyll-derived apocarotenoids decreased proportionally, which is in favor of the secondary formation of apo4 from apo3.

Analysis of Apocarotenoids in Roots

AGs were also analyzed in roots, which accumulate high amounts of β-carotene in response to *AtPSY* overexpression reflecting low activity of carotene hydroxylases (Maass et al., 2009). Although the aglycons of several well-known glycoconjugated precursors were released, such as coniferyl alcohol (from coniferin; Lewis and Yamamoto, 1990) and indol-3-acetonitril (from brassicin; Normanly and Bartel, 1999; Supplemental Fig. S11), we could not detect any AGs in either wild-type or *AtPSY*-overexpressing roots. Given the xanthophyll origin of the AGs identified, this may be attributed to the much lower xanthophyll abundance in roots than in leaves. This is contrasted by the presence of long-chain free β-apocarotenals in roots, which were up to 50-fold higher in *AtPSY*-overexpressing lines compared with the wild type (Fig. 5). As already mentioned above, these were not increased in leaves in response to increased pathway fluxes, indicating different mechanisms operating in both tissues.

DISCUSSION

Compensatory Responses toward Increased Carotenoid Flux in Arabidopsis Leaves

The carotenoid pathway capacity in Arabidopsis leaves is increased in response to the overexpression of the rate-limiting enzyme PSY. This is not at all evident from carotenoid levels but can be shown in derived nongreen cells, like calli and roots (Maass et al., 2009). Alternatively, phytoene accumulation upon NFZ inhibition can be used as a readout in leaves, because most carotenoid turnover apparently and conceivably happens downstream of phytoene. This revealed a doubling of phytoene amounts in *AtPSY*-overexpressing lines compared with wild-type leaves within 4 h of illumination with control light intensities (Fig. 1) and is further confirmed by in vitro measurements of PSY enzyme activity with isolated plastid membranes. Using these data, it can be estimated that wild-type leaf carotenoid homeostasis entails the de novo synthesis of about 14% of the carotenoids present (or 0.4 μg mg of dry weight^{-1}) during a 16-h light period, which is enhanced to 28% in *AtPSY*-overexpressing lines. The wild-type values match well with the carotenoid biosynthesis rate of 1.53 μg mg^{-1} within 48 h calculated for NFZ-treated pepper (*Capsicum annuum*) leaves (Simkin et al., 2003).

Only a portion of the overexpressed protein is membrane bound and contributes to flux increase, whereas the remainder resides in the stroma and cannot be active. Similar observations are known from daffodil chromoplasts, where an inactive stromal and an active membrane-bound population of PSY were found (Schledz et al., 1996; Bonk et al., 1997). Inactive stromal PSY was also observed in etiolated mustard (*Sinapis alba*) seedlings functioning as a sleeping enzyme pool that can rapidly be activated upon illumination by association to the developing membrane system (Welsch et al., 2000).

AGs are known aroma precursors identified in grapevine (Wirth et al., 2001) and various other fruits (Osorio et al., 1999, 2006; Winterhalter and Rouseff, 2001; Aubert et al., 2003), but they were not known from Arabidopsis hitherto. The major apocarotenoid aglycons identified here are apo1, apo2, apo3, and apo4. Interestingly, β-ionone supplemented to a *V. vinifera* cell culture is transformed into the same oxygenated AGs (Mathieu et al., 2009). Therefore, β-carotene represents a possible precursor, and in fact, $^{14}CO_2$ pulse-chase labeling experiments conducted with Arabidopsis pointed to α- and β-carotene as intermediates undergoing turnover; however, this study could not investigate xanthophyll turnover lacking sufficient label incorporation (Beisel et al., 2010).

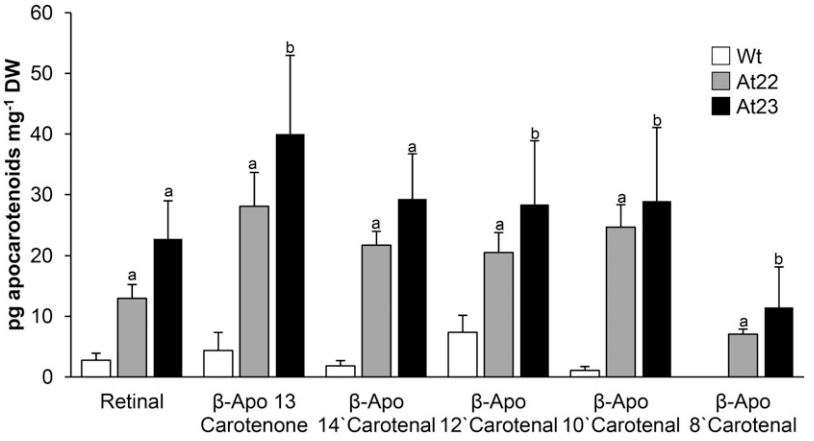

Figure 5. β-Apocarotenoids in Arabidopsis roots. β-Carotene-derived apocarotenoids were determined in roots from hydroponically grown plants from Arabidopsis wild-type (Wt; ecotype Wassilewskija) and two *AtPSY*-overexpressing (At22 and At23) lines by LC-MS analyses. Apocarotenoid amounts were quantified according to external standard curves and expressed in picograms per milligram of dry weight (DW). Data are mean ± SE of three biological replicates. a, Statistical significance (Student's *t* test, $P < 0.05$); b, statistical significance (Student's *t* test, $P < 0.1$).

Our data do not provide an indication for α- and β-carotenes contributing markedly to flux compensation by AG formation. In addition, although free β-carotene long-chain (nonglycosylated) cleavage products were detected, these did not increase upon flux acceleration (Supplemental Fig. S2). However, it cannot be excluded at this point that these compounds, antioxidants in their own right, are further degraded nonenzymatically or through catalysis by CCDs, some of which exhibit broad substrate and regional specificity of cleavage (Vogel et al., 2008; Ilg et al., 2009, 2014; Bruno et al., 2015). Hence, the free β-carotene-derived apocarotenoids detected may as well represent steady-state levels, like β-carotene itself. The fact that high light stress initiates the formation of β-carotene-derived cleavage products with signaling function (β-cyclocitral; Ramel et al., 2012b) witnesses that dynamic turnover occurs at the β-carotene level.

Xanthophylls Are Substrates for AGs

The AGs detected derive from a different path. As suggested by their structure containing in-ring hydroxyls and epoxy groups, they derive from xanthophylls (Fig. 3). The change in AG patterns responding according to the different proportions of xanthophylls present in carotenoid hydroxylase mutants (Fig. 4B) further supports their xanthophyll origin rather than an indirect route through secondary oxygenation of β-ionone (Mathieu et al., 2009). For instance, deficiency of the cytochrome P450 carotene hydroxylase CYP97A3 in *lut5* results in reduced levels of epoxyxanthophylls, like violaxanthin and neoxanthin. This correlated with lower levels of violaxanthin-derived apocarotenoid aglycons apo3 and apo4. The lower availability of these xanthophyll precursors thus entails their reduced degradation into AGs in *lut5*. Similarly, the absence of lutein caused by the deficiency of the only ε-ring-specific carotene hydroxylase CYP97C1 in the *lut1* mutant (Pogson et al., 1996; Kim et al., 2009) led to increased apo1 levels correlating with higher levels of zeinoxanthin and antheraxanthin, whereas other apocarotenoid aglycons remained unchanged. In addition, lutein can be excluded as precursor for any of the apocarotenoid aglycons, and its breakdown is expected to feed into different pathways.

AG accumulation also responds to increased pathway fluxes mediated by *AtPSY* overexpression. This can be concluded from increases of AGs and the biosynthetic capacity determined from phytoene amounts in the presence of NFZ with comparable rates (4-fold for AGs [Fig. 2C] and 3-fold for pathway flux [Fig. 1B]). Whether AG levels represent final sequestration forms or alternatively, are subjected to additional metabolic reactions remains to be investigated. Light is another factor capable in increasing pathway flux (Fig. 1B) and carotenoid degradation/turnover (Ramel et al., 2012a). However, the amounts of AGs did not change upon high light treatment of Arabidopsis leaves. In an interpretation, this is because of the fact that high light conditions activate violaxanthin deepoxidase as part of the xanthophyll cycle, which reduces the amounts of epoxidated xanthophylls considered as the primary AG precursors. Probably, the fast down-regulation determined for *CCD4* upon high light stress (Ramel et al., 2013) counteracts further reductions of epoxyxanthophylls and facilitates a fast increase in photoprotective zeaxanthin.

The formation of the AGs identified is not restricted to Arabidopsis; these compounds are known from fruits and grapevine (Wirth et al., 2001), suggesting broader relevance. None of the apocarotenoids identified could be traced back to the allenic moiety of neoxanthin. We did not detect its direct breakdown products (e.g. grasshopper ketone) or derivatives (e.g. β-damascenone), which are frequently observed in grapes and wines (Mendes-Pinto, 2009). Therefore, we suggest that the epoxidized β-xanthophylls antheraxanthin and violaxanthin are the prime source for AGs in Arabidopsis leaves. The much higher diversity of AGs found in fruits and flowers (Winterhalter and Rouseff, 2001; Brandi et al., 2011; Cooper et al., 2011) indicates changes in xanthophyll precursor utilization and secondary modifications, which might be related to enhanced xanthophyll breakdown accompanying fruit ripening or senescence.

CCD4 Is Mainly Responsible for AG Formation

The homogenous C_{13} backbone found in all AGs identified pleads for enzymatic cleavage of the xanthophyll precursor. CCD1 and CCD4 are the candidate cleavage oxygenases not contributing to abscisic acid and strigolactone biosynthesis and preferentially cleaving at C9 to C10 and C9′ to C10′ (Huang et al., 2009; Bruno et al., 2015), liberating a C_{13} backbone. In fact, the *ccd4-1* mutants showed low levels of all apocarotenoid aglycons, which were almost similar in the *ccd1-1 ccd4-1* double mutant. The homogeneous reduction of all apocarotenoids confirms the wide substrate specificity of CCD4 capable of cleaving all of the xanthophyll precursors suggested above and provides direct evidence of the enzymatic formation of the major proportion of AGs.

In *V. vinifera*, CCD1 was suggested to drive AG formation based on a correlation of *CCD1* expression with the formation of apocarotenoids, which were partially glycosylated during berry development (Mathieu et al., 2005). However, the transcripts from two grapevine *CCD4* genes were recently found to be similarly ripening induced (Lashbrooke et al., 2013). As stated above and despite similar substrate and product preferences of CCD1 and CCD4 in vitro (Vogel et al., 2008; Bruno et al., 2015), results from *ccd4-1* and *ccd1-1 ccd4-1* mutants are in favor of CCD4 being responsible for AG formation in planta. In agreement with this, CCD4 correlates with the formation of xanthophyll-derived apocarotenoids in two

yellow- and white-fleshed peach (*Prunus persica*) varieties (Brandi et al., 2011). White-fleshed fruits with high *CCD4* expression led to higher levels of, for example, apo3 compared with yellow-fleshed fruits. Furthermore, the suppression of *CCD4* results in higher xanthophyll amounts in *Ipomoea nil* and *C. morifolium* petals and potato (*Solanum tuberosum*) tubers (Ohmiya et al., 2006; Campbell et al., 2010; Yamamizo et al., 2010), and Arabidopsis *ccd4-1* knockout lines strongly increase their seed carotenoid contents (Gonzalez-Jorge et al., 2013).

The addition of sugar moieties is mediated by UDP glycosyltransferases, which exhibit wide substrate specificity. Their main function is to increase the solubility of toxic metabolites to allow their cellular transport for vacuolar sequestration (Ross et al., 2001). In fact, carotenoid breakdown products are often characterized by an electrophilic α,β-unsaturated moiety that can react further (Farmer and Mueller, 2013) and reported to cause various detrimental effects (concluded from animal model systems and enzyme inhibition assays; Ramel et al., 2012b). Recently, it was shown that apocarotenals are able to form adducts with proteins in vitro and therefore, have the potential to impair their functionality (Kalariya et al., 2011). Concluded from phytotoxicity studies, externally applied C_{13} apocarotenoids, including those identified in this work, inhibited seed germination and impaired root and shoot growth even at concentrations of 1 μM (D'Abrosca et al., 2004; DellaGreca et al., 2004). Apocarotenoid glycosylation may be one way to reduce this deleterious bioactivity of apocarotenoids generated during carotenoid steady-state regulation. This scenario may, however, be more complex. The crosses of *AtPSY*-overexpressing lines with *ccd4-1* and *ccd1-1 ccd4-1* were expected to produce fewer cleavage products, fewer AGs, and hence, increased leaf carotenoid levels. The lethal seedling obtained, however, points to deleterious effects at high fluxes when the detoxification pathway into AGs is dysfunctional. Possibly, nonenzymatic degradation takes over, leading to an uncoordinated accumulation of free cleavage products, which by yet unknown mechanisms, do not find their way toward glycosylation. Possibly, as mentioned above, detoxification of carotenoid breakdown products by glycosylation might require the coordinated supply of glycosidases. The recent detection of CCD4 localized in carotenoid-bearing plastoglubules might point toward an involvement of these plastid structures in carotenoid breakdown and their subsequent metabolization (Ytterberg et al., 2006; Rubio et al., 2008).

Tissue-Specific Differences in Carotenoid Degradation

There are tissue-dependent differences in carotenoid accumulation upon *PSY* overexpression. Although leaves maintain steady-state levels, nongreen cells, like roots and calli, accumulate β-carotene to an extent that crystals form (Maass et al., 2009). Apparently, carotene hydroxylation becomes rate limiting upon enhanced pathway flux and determines the amounts of β-carotene accumulating. Thus, it is the low amount of xanthophylls present in Arabidopsis roots that causes the absence of AGs; this again corroborates their xanthophyll origin. Interestingly, coexpression of a hydroxylase gene in *PSY*-overexpressing citrus callus dramatically reduces its β-carotene content but does not equivalently increase total xanthophyll amounts (Cao et al., 2012). It remains to be determined whether this is because of increased xanthophyll cleavage or an accumulation of AGs.

While AGs are absent, Arabidopsis roots accumulate nonglycosylated long-chain β-carotene-derived apocarotenoids (Fig. 5) and respond positively to *AtPSY* overexpression, which is in contrast to leaves. However, all β-apocarotenals identified make up only about 0.03% of the β-carotene amount accumulating in the transgenic roots. This may be because of the crystalline form of β-carotene, a mode of deposition also met in carrots (*Daucus carota*), tomato, and papaya (*Carica papaya*; Kim et al., 2010; Schweiggert et al., 2011). These molecules are not in monodisperse solution and are assumed to be in a more stable form, being protected from both enzymatic degradation and possible radical attack. A similar stabilizing effect was suggested also for crystalline lycopene in tomato chromoplasts (Nogueira et al., 2013).

Therefore, additional reduction of carotene hydroxylation seems to be the most promising approach to improve β-carotene (provitamin A) accumulation in crops that accumulate xanthophylls in addition to carotenes. In fact, this is observed in association with a widespread CYP97A3 deficiency in orange carrot cultivars (Arango et al., 2014) and favorable BCH alleles in maize (*Zea mays*; Yan et al., 2010) as well as in biotechnological approaches (e.g. in potato tubers; Diretto et al., 2007). Approaches combining both a reduced β-carotene metabolization by inhibiting carotene hydroxylation and an increased pathway flux by higher levels of PSY are, therefore, expected to further boost the development of crops with provitamin A-enriched tissues.

MATERIALS AND METHODS

In Vitro PSY Activity

Plastid isolation from leaves of 4-week-old Arabidopsis (*Arabidopsis thaliana*) plants was performed according to the work by Welsch et al. (2000). Pellets were resuspended in 2 mL of lysis buffer (20 mM Tris, pH 8.0 and 4 mM $MgCl_2$), incubated on ice for 10 min, and separated into stroma and membrane fractions by centrifugation at 21,000*g* for 10 min. Membranes were resuspended in 300 μL of lysis buffer, and protein concentration was determined using the Bio-Rad Protein Assay (Bio-Rad). For in vitro phytoene synthesis, 200 μg of protein was incubated with 10 μM [^{14}C]isopentenyl diphosphate (50 mCi mmol^{-1}; ARC), 20 μM [^{14}C]isopentenyl diphosphate, 40 μM dimethylallyl diphosphate (isoprenoids), 4 mM ATP, and 10 μg of recombinant purified geranylgeranyl diphosphate synthase (Kloer et al., 2006) for 30 min. Incubation conditions and product analysis and quantification were performed by scintillation counting and thin-layer chromatography scanning as described (Welsch et al., 2000).

^{14}C-Labeling Experiments

^{14}C labeling was performed essentially according to the work by Beisel et al. (2010). Basically, $^{14}CO_2$ was liberated from [^{14}C]carbonate solution by acid and heat and applied to detached rosette leaves placed in a leaf chamber.

After 30 min in growth light (pulse period; approximately 130 μmol photons m^{-2} s^{-1}), remaining $^{14}CO_2$ was adsorbed, the chamber was opened, and the leaves were subsequently exposed to strong light for 30 min (chase period; approximately 1,000 μmol photons m^{-2} s^{-1}). ^{14}C incorporation into β-carotene (all isomers) was analyzed upon extraction with acetone by radio-HPLC as described (Beisel et al., 2010).

Carotenoid Analysis

Carotenoids were extracted using lyophilized leaves and analyzed by HPLC as described (Welsch et al., 2008).

LC-MS Analysis

In total, 500 mg (roots) or 10 mg (leaves) of lyophilized powder was extracted three times with 2 mL of acetone. Supernatants were combined and spiked with 60 μL of each external standard VIS682A (QCR Solutions; 20 μg mL^{-1}); 2 mL of petroleum ether:diethyl ether (1:4, v/v) was added, filled up to 14 mL with water, and centrifuged for 5 min at 4,000*g*. The hyperphase was transferred into a new tube, and extraction was repeated one time. Combined petroleum ether and diethyl ether supernatants were dried in a vortex evaporator and redissolved in $CHCl_3$:MeOH (1:1, v/v; 60 μL for root extracts and 100 μL for leaf extracts), and 2 μL was injected into the LC-MS system consisting of an Orbitrap-based Thermo Q-Exactive coupled to a Thermo Ultimate 3000 UPLC System (Thermo Scientific). Separation was performed with a C_{18} UPLC Column (Hypersil Gold 150 × 2.1 mm, 1.9 μm; Thermo Scientific) using solvent systems A (water + 0.05% [v/v] acetic acid) and B (acetonitrile + 0.05% [v/v] acetic acid). The column was developed with a flow rate of 0.5 mL min^{-1} of isocratic for 1 min followed by a linear gradient from 70% B to 100% B within 5 min maintained for 10 min and then, to 70% B within 3 min, maintaining the final conditions for another 4 min. Identification of apocarotenoids was carried out using atmospheric pressure chemical ionization in positive mode. Nitrogen was used as sheath and auxiliary gas (set to 20 and 10 arbitrary units, respectively). Vaporizer temperature was set to 350°C, and capillary temperature was 320°C. Spray voltage was set to 5 kV, and normalized collision energy was set to 35 arbitrary units. Data analysis was performed using the TraceFinder 3.1 software (Thermo Scientific). Quantification of apocarotenoids was performed with external calibration curves using the following authentic apocarotenoid standards: β-apo-13-carotenone ($C_{18}H_{26}O$; mass-to-charge ratio [*m/z*] = 258.19836), retinal ($C_{20}H_{28}O$; *m/z* = 284.21401), β-apo-14′-carotenal ($C_{22}H_{30}O$; *m/z* = 310.22966), β-apo-12′-carotenal ($C_{25}H_{34}O$; *m/z* = 350.26096), β-apo-10′-carotenal ($C_{27}H_{36}O$; *m/z* = 376.27661), and β-apo-8′-carotenal ($C_{30}H_{40}O$, *m/z* = 416.30791). The internal standard VIS682A detected at 682 nm was used to correct for injection errors and volume variations.

Analysis of AGs

Protocols for Arabidopsis were based on extraction procedure of AGs for grapevine (*Vitis vinifera*; Wirth et al., 2001; Mathieu et al., 2005). Leaves (5 g) from 4-week-old Arabidopsis plants were ground in liquid nitrogen and incubated in 50 mL of 40 mM gluconolactone in water to inhibit endogenous glycosidases. After 90 min of continuous shaking, samples were centrifuged (15 min at 6,000*g*), and the supernatant was filtered using Grade GF/C Glass Microfiber Filters (Whatman). Sep-Pac Columns (C18; Waters) were conditioned with 10 mL of MeOH, equilibrated with 10 mL of water, and samples were loaded onto the columns, washed with 10 mL of water, and eluted with 10 mL of MeOH. Eluates were dried in a rotary evaporator, resuspended in 400 μL of citrate buffer (0.1 M Na_2HPO_4 and 0.05 M citric acid, pH 5.0), and distributed into two aliquots with 200 μL each. One aliquot was incubated with 100 μL of 10 mg mL^{-1} rapidase AR200 (DSM) in citrate buffer and incubated at 40°C overnight with shaking at 250 rpm. The second aliquot was used as a nondigested control and processed similarly. Samples were mixed with 100 μL of pentane:dichloromethane (2:1, v/v) and centrifuged at 21,500*g* for 10 min, and the upper pentane layer was transferred into a fresh tube. Extraction was repeated two times, the pentane phases were combined, 50 μL of the internal standard 4-nonanol (625 ng μL^{-1} in ethanol) was added, and the volume was reduced to 100 μL under a stream of nitrogen and stored at −20°C until analysis. Root extracts were prepared accordingly from 5 g of roots from hydroponically grown Arabidopsis plants (Hétu et al., 2005).

GC-MS analyses were performed on a Trace GC/Trace DSQII System (Thermo). The instrument was equipped with a 30-m Zebron ZB5 Column (30 m × 0.25 mm × 0.25 μm; Phenomenex), and the velocity of the carrier gas (He) was at 1 mL min^{-1}. Injections of 2 μL of the extracts were carried out in splitless mode, and the injector temperature was set at 220°C. Oven temperature was initially set at 60°C for 5 min, then progressed at a rate of 25°C min^{-1} to 340°C, and maintained for 5 min. Ionization was performed in electron impact mode (70 eV). Initially, acquisition was performed in scan mode to identify apocarotenoids using the NIST2005 Mass Spectral Library (National Institute of Standards). Compound identity was confirmed in positive ion chemical ionization mode by comparing retention time of molecule ion mass with ion spectra from electron impact analysis of the same samples. Quantification was done on selected daughter ions (152 *m/z* for apo1, 150 *m/z* for apo2, 123 *m/z* for apo3, 124 *m/z* for apo4, and 101 *m/z* for the internal standard 4-nonanol). Nonisothermal Kovats indices were calculated according to the work by Vandendool and Kratz (1963).

Immunoblot Analysis

Generation and affinity purification of antibodies directed against Arabidopsis PSY is described in the work by Maass et al. (2009). Proteins were extracted with phenol from plastids and plastid subfractions as described (Welsch et al., 2007). After SDS-PAGE, blotting onto polyvinylidene difluoride membranes (Carl Roth), and treatment with blocking solution (Tris-buffered saline containing 5% [w/v] milk powder), membranes were incubated with antibodies in Tris-buffered saline containing 0.1% (v/v) Tween 20 and 1% (w/v) milk powder. For detection, the ECL System (GE Healthcare) was used. An SDS gel with the same protein amounts was stained with Coomassie to confirm equal loading of proteins.

Arabidopsis Growth

Arabidopsis seeds were grown on soil at 20°C under long-day conditions with 100 μmol photons m^{-2} s^{-1}. For high light treatment, plants were illuminated with 1,500 μmol photons m^{-2} s^{-1} for 4 h at 21°C. Corresponding background Arabidopsis ecotype was used for experiments with *AtPSY*-overexpressing lines (Wassilewskija) and *CCD* and carotene hydroxylase mutants (Columbia-0).

NFZ treatments were done according to the work by Beisel et al. (2011). Leaves from 4-week-old plants were detached, immediately transferred onto 70 mM NFZ, and incubated for 2 h in the dark. Leaves were transferred onto 10 mM NFZ and further incubated for 4 h with 100 μmol photons m^{-2} s^{-1}. Leaves were always incubated with the adaxial surface facing the air. Leaves were harvested immediately, frozen in liquid nitrogen, and lyophilized, and carotenoids were extracted and analyzed by HPLC.

The transfer DNA knockout line for *CYP97C1* (At3g53130, SALK_129724, *lut1-4*) was obtained from the Arabidopsis Biological Resource Center, and the lines for *CYP97A3* (At1g31800, *lut5-1*), *CCD4* (At4g19170, SALK_097984, *ccd4-1*), and a double mutant from a cross with *ccd1-1* (At3g63520, SAIL_390_C01) were provided by Dean DellaPenna.

Supplemental Data

The following supplemental materials are available.

Supplemental Figure S1. [^{14}C]-Labeled compounds formed in an in vitro PSY activity assay.

Supplemental Figure S2. β-Apocarotenoids in Arabidopsis leaves.

Supplemental Figure S3. Identification of apo1 in glycosidase-digested Arabidopsis wild-type leaf extracts by GC-MS analysis.

Supplemental Figure S4. Identification of apo2 in glycosidase-digested Arabidopsis wild-type leaf extracts by GC-MS analysis.

Supplemental Figure S5. Identification of apo3 in glycosidase-digested Arabidopsis wild-type leaf extracts by GC-MS analysis.

Supplemental Figure S6. Identification of apo4 in glycosidase-digested Arabidopsis wild-type leaf extracts by GC-MS analysis.

Supplemental Figure S7. AGs in *AtPSY*-overexpressing Arabidopsis leaves.

Supplemental Figure S8. AGs in leaves from Arabidopsis *CCD4* mutant.

Supplemental Figure S9. Crosses between *AtPSY*-overexpressing and *ccd4-1* mutant Arabidopsis lines.

Supplemental Figure S10. Apocarotenoid aglycons in leaves from Arabidopsis carotene hydroxylase mutants.

Supplemental Figure S11. Identification of coniferyl alcohol and indol-3-acetonitril in glycosidase-digested Arabidopsis wild-type root extracts by GC-MS analysis.

Supplemental Table S1. Characteristics of apocarotenoid aglycons identified in Arabidopsis leaves.

ACKNOWLEDGMENTS

We thank Dean DellaPenna (Michigan State University) for providing seeds of hydroxylase and *CCD* mutant lines, Mark Bruno (University of Freiburg) for valuable discussions, and Carmen Schubert (University of Freiburg) for skillful assistance.

Received February 16, 2015; accepted June 25, 2015; published July 1, 2015.

LITERATURE CITED

Aharoni A, Giri AP, Deuerlein S, Griepink F, de Kogel WJ, Verstappen FWA, Verhoeven HA, Jongsma MA, Schwab W, Bouwmeester HJ (2003) Terpenoid metabolism in wild-type and transgenic *Arabidopsis* plants. Plant Cell **15:** 2866–2884

Alder A, Jamil M, Marzorati M, Bruno M, Vermathen M, Bigler P, Ghisla S, Bouwmeester H, Beyer P, Al-Babili S (2012) The path from β-carotene to carlactone, a strigolactone-like plant hormone. Science **335:** 1348–1351

Arango J, Jourdan M, Geoffriau E, Beyer P, Welsch R (2014) Carotene hydroxylase activity determines the levels of both α-carotene and total carotenoids in orange carrots. Plant Cell **26:** 2223–2233

Aubert C, Ambid C, Baumes R, Günata Z (2003) Investigation of bound aroma constituents of yellow-fleshed nectarines (*Prunus persica* L. Cv. Springbright). changes in bound aroma profile during maturation. J Agric Food Chem **51:** 6280–6286

Auldridge ME, Block A, Vogel JT, Dabney-Smith C, Mila I, Bouzayen M, Magallanes-Lundback M, DellaPenna D, McCarty DR, Klee HJ (2006) Characterization of three members of the Arabidopsis carotenoid cleavage dioxygenase family demonstrates the divergent roles of this multifunctional enzyme family. Plant J **45:** 982–993

Avendaño-Vázquez AO, Cordoba E, Llamas E, San Román C, Nisar N, De la Torre S, Ramos-Vega M, Gutiérrez-Nava MD, Cazzonelli CI, Pogson BJ, et al (2014) An uncharacterized apocarotenoid-derived signal generated in ζ-carotene desaturase mutants regulates leaf development and the expression of chloroplast and nuclear genes in *Arabidopsis*. Plant Cell **26:** 2524–2537

Ballottari M, Alcocer MJP, D'Andrea C, Viola D, Ahn TK, Petrozza A, Polli D, Fleming GR, Cerullo G, Bassi R (2014) Regulation of photosystem I light harvesting by zeaxanthin. Proc Natl Acad Sci USA **111:** E2431–E2438

Beisel KG, Jahnke S, Hofmann D, Köppchen S, Schurr U, Matsubara S (2010) Continuous turnover of carotenes and chlorophyll *a* in mature leaves of Arabidopsis revealed by $^{14}CO_2$ pulse-chase labeling. Plant Physiol **152:** 2188–2199

Beisel KG, Schurr U, Matsubara S (2011) Altered turnover of β-carotene and Chl a in Arabidopsis leaves treated with lincomycin or norflurazon. Plant Cell Physiol **52:** 1193–1203

Bonk M, Hoffmann B, Von Lintig J, Schledz M, Al-Babili S, Hobeika E, Kleinig H, Beyer P (1997) Chloroplast import of four carotenoid biosynthetic enzymes in vitro reveals differential fates prior to membrane binding and oligomeric assembly. Eur J Biochem **247:** 942–950

Brandi F, Bar E, Mourgues F, Horváth G, Turcsi E, Giuliano G, Liverani A, Tartarini S, Lewinsohn E, Rosati C (2011) Study of 'Redhaven' peach and its white-fleshed mutant suggests a key role of CCD4 carotenoid dioxygenase in carotenoid and norisoprenoid volatile metabolism. BMC Plant Biol **11:** 24

Bruno M, Beyer P, Al-Babili S (2015) The potato carotenoid cleavage dioxygenase 4 catalyzes a single cleavage of β-ionone ring-containing carotenes and non-epoxidated xanthophylls. Arch Biochem Biophys **572:** 126–133

Bruno M, Hofmann M, Vermathen M, Alder A, Beyer P, Al-Babili S (2014) On the substrate- and stereospecificity of the plant carotenoid cleavage dioxygenase 7. FEBS Lett **588:** 1802–1807

Busch M, Seuter A, Hain R (2002) Functional analysis of the early steps of carotenoid biosynthesis in tobacco. Plant Physiol **128:** 439–453

Campbell R, Ducreux LJM, Morris WL, Morris JA, Suttle JC, Ramsay G, Bryan GJ, Hedley PE, Taylor MA (2010) The metabolic and developmental roles of Carotenoid Cleavage Dioxygenase4 from potato. Plant Physiol **154:** 656–664

Cao H, Zhang J, Xu J, Ye J, Yun Z, Xu Q, Xu J, Deng X (2012) Comprehending crystalline β-carotene accumulation by comparing engineered cell models and the natural carotenoid-rich system of citrus. J Exp Bot **63:** 4403–4417

Chen Y, Li F, Wurtzel ET (2010) Isolation and characterization of the *Z-ISO* gene encoding a missing component of carotenoid biosynthesis in plants. Plant Physiol **153:** 66–79

Cooper CM, Davies NW, Motti CA, Menary RC (2011) Glycosidic conjugates of C13 norisoprenoids, monoterpenoids, and cucurbates in *Boronia megastigma* (Nees). J Agric Food Chem **59:** 2610–2617

D'Abrosca B, DellaGreca M, Fiorentino A, Monaco P, Oriano P, Temussi F (2004) Structure elucidation and phytotoxicity of C13 nor-isoprenoids from *Cestrum parqui*. Phytochemistry **65:** 497–505

DellaGreca M, Di Marino C, Zarrelli A, D'Abrosca B (2004) Isolation and phytotoxicity of apocarotenoids from *Chenopodium album*. J Nat Prod **67:** 1492–1495

Demmig-Adams B, Adams WW III (2002) Antioxidants in photosynthesis and human nutrition. Science **298:** 2149–2153

Diretto G, Welsch R, Tavazza R, Mourgues F, Pizzichini D, Beyer P, Giuliano G (2007) Silencing of beta-carotene hydroxylase increases total carotenoid and beta-carotene levels in potato tubers. BMC Plant Biol **7:** 11

Egea I, Barsan C, Bian W, Purgatto E, Latché A, Chervin C, Bouzayen M, Pech JC (2010) Chromoplast differentiation: current status and perspectives. Plant Cell Physiol **51:** 1601–1611

Enzell C (1985) Biodegradation of carotenoids: an important route to aroma compounds. Pure Appl Chem **57:** 693–700

Farmer EE, Mueller MJ (2013) ROS-mediated lipid peroxidation and RES-activated signaling. Annu Rev Plant Biol **64:** 429–450

Fraser PD, Römer S, Shipton CA, Mills PB, Kiano JW, Misawa N, Drake RG, Schuch W, Bramley PM (2002) Evaluation of transgenic tomato plants expressing an additional phytoene synthase in a fruit-specific manner. Proc Natl Acad Sci USA **99:** 1092–1097

Fray RG, Wallace A, Fraser PD, Valero D, Hedden P, Bramley PM, Grierson D (1995) Constitutive expression of a fruit phytoene synthase gene in transgenic tomatoes causes dwarfism by redirecting metabolites from the gibberellin pathway. Plant J **8:** 693–701

Frusciante S, Diretto G, Bruno M, Ferrante P, Pietrella M, Prado-Cabrero A, Rubio-Moraga A, Beyer P, Gomez-Gomez L, Al-Babili S, et al (2014) Novel carotenoid cleavage dioxygenase catalyzes the first dedicated step in saffron crocin biosynthesis. Proc Natl Acad Sci USA **111:** 12246–12251

Gonzalez-Jorge S, Ha SH, Magallanes-Lundback M, Gilliland LU, Zhou A, Lipka AE, Nguyen YN, Angelovici R, Lin H, Cepela J, et al (2013) Carotenoid Cleavage Dioxygenase4 is a negative regulator of β-carotene content in *Arabidopsis* seeds. Plant Cell **25:** 4812–4826

Havaux M (2014) Carotenoid oxidation products as stress signals in plants. Plant J **79:** 597–606

Hétu MF, Tremblay LJ, Lefebvre DD (2005) High root biomass production in anchored Arabidopsis plants grown in axenic sucrose supplemented liquid culture. Biotechniques **39:** 345–349

Huang FC, Horváth G, Molnár P, Turcsi E, Deli J, Schrader J, Sandmann G, Schmidt H, Schwab W (2009) Substrate promiscuity of RdCCD1, a carotenoid cleavage oxygenase from *Rosa damascena*. Phytochemistry **70:** 457–464

Ilg A, Beyer P, Al-Babili S (2009) Characterization of the rice carotenoid cleavage dioxygenase 1 reveals a novel route for geranial biosynthesis. FEBS J **276:** 736–747

Ilg A, Bruno M, Beyer P, Al-Babili S (2014) Tomato carotenoid cleavage dioxygenases 1A and 1B: relaxed double bond specificity leads to a plenitude of dialdehydes, mono-apocarotenoids and isoprenoid volatiles. FEBS Open Bio **4:** 584–593

Isaacson T, Ronen G, Zamir D, Hirschberg J (2002) Cloning of *tangerine* from tomato reveals a carotenoid isomerase essential for the production of beta-carotene and xanthophylls in plants. Plant Cell **14:** 333–342

Iuchi S, Kobayashi M, Taji T, Naramoto M, Seki M, Kato T, Tabata S, Kakubari Y, Yamaguchi-Shinozaki K, Shinozaki K (2001) Regulation

of drought tolerance by gene manipulation of 9-cis-epoxycarotenoid dioxygenase, a key enzyme in abscisic acid biosynthesis in Arabidopsis. Plant J **27:** 325–333

Kalariya NM, Ramana KV, Srivastava SK, van Kuijk FJGM (2011) Post-translational protein modification by carotenoid cleavage products. Biofactors **37:** 104–116

Kim J, DellaPenna D (2006) Defining the primary route for lutein synthesis in plants: the role of Arabidopsis carotenoid beta-ring hydroxylase CYP97A3. Proc Natl Acad Sci USA **103:** 3474–3479

Kim J, Smith JJ, Tian L, Dellapenna D (2009) The evolution and function of carotenoid hydroxylases in Arabidopsis. Plant Cell Physiol **50:** 463–479

Kim JE, Rensing KH, Douglas CJ, Cheng KM (2010) Chromoplasts ultrastructure and estimated carotene content in root secondary phloem of different carrot varieties. Planta **231:** 549–558

Kloer DP, Welsch R, Beyer P, Schulz GE (2006) Structure and reaction geometry of geranylgeranyl diphosphate synthase from *Sinapis alba*. Biochemistry **45:** 15197–15204

Lashbrooke JG, Young PR, Dockrall SJ, Vasanth K, Vivier MA (2013) Functional characterisation of three members of the *Vitis vinifera* L. carotenoid cleavage dioxygenase gene family. BMC Plant Biol **13:** 156

Lewis NG, Yamamoto E (1990) Lignin: occurrence, biogenesis and biodegradation. Annu Rev Plant Physiol Plant Mol Biol **41:** 455–496

Li F, Vallabhaneni R, Wurtzel ET (2008) *PSY3*, a new member of the phytoene synthase gene family conserved in the *Poaceae* and regulator of abiotic stress-induced root carotenogenesis. Plant Physiol **146:** 1333–1345

Maass D, Arango J, Wüst F, Beyer P, Welsch R (2009) Carotenoid crystal formation in Arabidopsis and carrot roots caused by increased phytoene synthase protein levels. PLoS One **4:** e6373

Mathieu S, Terrier N, Procureur J, Bigey F, Günata Z (2005) A carotenoid cleavage dioxygenase from *Vitis vinifera* L.: functional characterization and expression during grape berry development in relation to C13-norisoprenoid accumulation. J Exp Bot **56:** 2721–2731

Mathieu S, Wirth J, Sauvage FX, Lepoutre JP, Baumes R, Gunata Z (2009) Biotransformation of C13-norisoprenoids and monoterpenes by a cell suspension culture of cv. Gamay (*Vitis vinifera*). Plant Cell Tissue Organ Cult **97:** 203–213

Mendes-Pinto MM (2009) Carotenoid breakdown products the-norisoprenoids-in wine aroma. Arch Biochem Biophys **483:** 236–245

Nisar N, Li L, Lu S, Khin NC, Pogson BJ (2015) Carotenoid metabolism in plants. Mol Plant **8:** 68–82

Niyogi KK (1999) Photoprotection revisited: genetic and molecular approaches. Annu Rev Plant Physiol Plant Mol Biol **50:** 333–359

Nogueira M, Mora L, Enfissi EMA, Bramley PM, Fraser PD (2013) Subchromoplast sequestration of carotenoids affects regulatory mechanisms in tomato lines expressing different carotenoid gene combinations. Plant Cell **25:** 4560–4579

Normanly J, Bartel B (1999) Redundancy as a way of life: IAA metabolism. Curr Opin Plant Biol **2:** 207–213

Ohmiya A, Kishimoto S, Aida R, Yoshioka S, Sumitomo K (2006) Carotenoid cleavage dioxygenase (CmCCD4a) contributes to white color formation in chrysanthemum petals. Plant Physiol **142:** 1193–1201

Osorio C, Alarcon M, Moreno C, Bonilla A, Barrios J, Garzon C, Duque C (2006) Characterization of odor-active volatiles in champa (*Campomanesia lineatifolia* R. and P.). J Agric Food Chem **54:** 509–516

Osorio C, Duque C, Fujimoto Y (1999) C(13)-Norisoprenoid glucoconjugates from lulo (*Solanum quitoense* L.) leaves. J Agric Food Chem **47:** 1641–1645

Park H, Kreunen SS, Cuttriss AJ, DellaPenna D, Pogson BJ (2002) Identification of the carotenoid isomerase provides insight into carotenoid biosynthesis, prolamellar body formation, and photomorphogenesis. Plant Cell **14:** 321–332

Pogson B, McDonald KA, Truong M, Britton G, DellaPenna D (1996) *Arabidopsis* carotenoid mutants demonstrate that lutein is not essential for photosynthesis in higher plants. Plant Cell **8:** 1627–1639

Ramel F, Birtic S, Cuiné S, Triantaphylidès C, Ravanat JL, Havaux M (2012a) Chemical quenching of singlet oxygen by carotenoids in plants. Plant Physiol **158:** 1267–1278

Ramel F, Birtic S, Ginies C, Soubigou-Taconnat L, Triantaphylidès C, Havaux M (2012b) Carotenoid oxidation products are stress signals that mediate gene responses to singlet oxygen in plants. Proc Natl Acad Sci USA **109:** 5535–5540

Ramel F, Mialoundama AS, Havaux M (2013) Nonenzymic carotenoid oxidation and photooxidative stress signalling in plants. J Exp Bot **64:** 799–805

Rodrigo MJ, Alquézar B, Alós E, Medina V, Carmona L, Bruno M, Al-Babili S, Zacarías L (2013) A novel carotenoid cleavage activity involved in the biosynthesis of Citrus fruit-specific apocarotenoid pigments. J Exp Bot **64:** 4461–4478

Rodríguez-Villalón A, Gas E, Rodríguez-Concepción M (2009) Phytoene synthase activity controls the biosynthesis of carotenoids and the supply of their metabolic precursors in dark-grown Arabidopsis seedlings. Plant J **60:** 424–435

Ross J, Li Y, Lim EK, Bowles D (2001) Higher plant glycosyltransferases. Genome Biol **2:** REVIEWS3004

Rubio A, Rambla JL, Santaella M, Gómez MD, Orzaez D, Granell A, Gómez-Gómez L (2008) Cytosolic and plastoglobule-targeted carotenoid dioxygenases from *Crocus sativus* are both involved in beta-ionone release. J Biol Chem **283:** 24816–24825

Ruiz-Sola MÁ, Rodríguez-Concepción M (2012) Carotenoid biosynthesis in Arabidopsis: a colorful pathway. Arabidopsis Book **10:** e0158

Schledz M, al-Babili S, von Lintig J, Haubruck H, Rabbani S, Kleinig H, Beyer P (1996) Phytoene synthase from *Narcissus pseudonarcissus*: functional expression, galactolipid requirement, topological distribution in chromoplasts and induction during flowering. Plant J **10:** 781–792

Schweiggert RM, Steingass CB, Heller A, Esquivel P, Carle R (2011) Characterization of chromoplasts and carotenoids of red- and yellow-fleshed papaya (*Carica papaya* L.). Planta **234:** 1031–1044

Shewmaker CK, Sheehy JA, Daley M, Colburn S, Ke DY (1999) Seed-specific overexpression of phytoene synthase: increase in carotenoids and other metabolic effects. Plant J **20:** 401–412X

Simkin AJ, Schwartz SH, Auldridge M, Taylor MG, Klee HJ (2004) The tomato carotenoid cleavage dioxygenase 1 genes contribute to the formation of the flavor volatiles beta-ionone, pseudoionone, and geranylacetone. Plant J **40:** 882–892

Simkin AJ, Zhu C, Kuntz M, Sandmann G (2003) Light-dark regulation of carotenoid biosynthesis in pepper (*Capsicum annuum*) leaves. J Plant Physiol **160:** 439–443

Sitte P, Falk H, Liedvogel B (1980) Chromoplasts. *In* FC Czygan, ed, Pigment Plants, Ed 2. Fischer, Stuttgart, Germany, pp 117–148

Tan BC, Joseph LM, Deng WT, Liu L, Li QB, Cline K, McCarty DR (2003) Molecular characterization of the Arabidopsis 9-cis epoxycarotenoid dioxygenase gene family. Plant J **35:** 44–56

Vandendool H, Kratz PD (1963) A generalization of the retention index system including linear temperature programmed gas-liquid partition chromatography. J Chromatogr A **11:** 463–471

Vogel JT, Tan BC, McCarty DR, Klee HJ (2008) The carotenoid cleavage dioxygenase 1 enzyme has broad substrate specificity, cleaving multiple carotenoids at two different bond positions. J Biol Chem **283:** 11364–11373

von Lintig J, Welsch R, Bonk M, Giuliano G, Batschauer A, Kleinig H (1997) Light-dependent regulation of carotenoid biosynthesis occurs at the level of phytoene synthase expression and is mediated by phytochrome in *Sinapis alba* and *Arabidopsis thaliana* seedlings. Plant J **12:** 625–634

Welsch R, Arango J, Bär C, Salazar B, Al-Babili S, Beltrán J, Chavarriaga P, Ceballos H, Tohme J, Beyer P (2010) Provitamin A accumulation in cassava (*Manihot esculenta*) roots driven by a single nucleotide polymorphism in a phytoene synthase gene. Plant Cell **22:** 3348–3356

Welsch R, Beyer P, Hugueney P, Kleinig H, von Lintig J (2000) Regulation and activation of phytoene synthase, a key enzyme in carotenoid biosynthesis, during photomorphogenesis. Planta **211:** 846–854

Welsch R, Maass D, Voegel T, Dellapenna D, Beyer P (2007) Transcription factor RAP2.2 and its interacting partner SINAT2: stable elements in the carotenogenesis of Arabidopsis leaves. Plant Physiol **145:** 1073–1085

Welsch R, Wüst F, Bär C, Al-Babili S, Beyer P (2008) A third phytoene synthase is devoted to abiotic stress-induced abscisic acid formation in rice and defines functional diversification of phytoene synthase genes. Plant Physiol **147:** 367–380

Winterhalter P, Rouseff RL (2001) Carotenoid-derived aroma compounds: an introduction. *In* P Winterhalter, RL Rouseff, eds, Carotenoid Aroma Compounds. ACS Symposium Series, American Chemical Society, Washington, DC,. pp 1–17

Winterhalter P, Schreier P (1995) The generation of norisoprenoid volatiles in starfruit (*Averrhoa carambola* L.): a review. Food Rev Int **11:** 237–254

Winterhalter P, Skouroumounis GK (1997) Glycoconjugated aroma compounds: occurrence, role and biotechnological transformation. Adv Biochem Eng Biotechnol **55:** 73–105

Wirth J, Guo W, Baumes R, Günata Z (2001) Volatile compounds released by enzymatic hydrolysis of glycoconjugates of leaves and grape berries from *Vitis vinifera* Muscat of Alexandria and Shiraz cultivars. J Agric Food Chem **49:** 2917–2923

Yamamizo C, Kishimoto S, Ohmiya A (2010) Carotenoid composition and carotenogenic gene expression during *Ipomoea petal* development. J Exp Bot **61:** 709–719

Yan J, Kandianis CB, Harjes CE, Bai L, Kim EH, Yang X, Skinner DJ, Fu Z, Mitchell S, Li Q, et al (2010) Rare genetic variation at *Zea mays crtRB1* increases beta-carotene in maize grain. Nat Genet **42:** 322–327

Ye X, Al-Babili S, Klöti A, Zhang J, Lucca P, Beyer P, Potrykus I (2000) Engineering the provitamin A (β-carotene) biosynthetic pathway into (carotenoid-free) rice endosperm. Science **287:** 303–305

Ytterberg AJ, Peltier JB, van Wijk KJ (2006) Protein profiling of plastoglobules in chloroplasts and chromoplasts: a surprising site for differential accumulation of metabolic enzymes. Plant Physiol **140:** 984–997

Yu Q, Ghisla S, Hirschberg J, Mann V, Beyer P (2011) Plant carotene cis-trans isomerase CRTISO: a new member of the FAD(RED)-dependent flavoproteins catalyzing non-redox reactions. J Biol Chem **286:** 8666–8676

Zhou X, Welsch R, Yang Y, Álvarez D, Riediger M, Yuan H, Fish T, Liu J, Thannhauser TW, Li L (2015) Arabidopsis OR proteins are the major posttranscriptional regulators of phytoene synthase in controlling carotenoid biosynthesis. Proc Natl Acad Sci USA **112:** 3558–3563